IC/93/412

INTERNATIONAL CENTRE FOR
THEORETICAL PHYSICS

TUNNELING OF SELF-TRAPPED STATES AND FORMATION OF A BAND

K. Yonemitsu

INTERNATIONAL
ATOMIC ENERGY
AGENCY

UNITED NATIONS
EDUCATIONAL,
SCIENTIFIC
AND CULTURAL
ORGANIZATION

MIRAMARE-TRIESTE

IC/93/412

International Atomic Energy Agency
and
United Nations Educational Scientific and Cultural Organization
INTERNATIONAL CENTRE FOR THEORETICAL PHYSICS

TUNNELING OF SELF-TRAPPED STATES AND FORMATION OF A BAND

K. Yonemitsu
International Centre for Theoretical Physics, Trieste, Italy.

MIRAMARE – TRIESTE
December 1993

Tunneling of a self-trapped kink and formation of a band are studied semiclassically in the one-dimensional extended Peierls-Hubbard model near half filling. We consider up to Gaussian fluctuations around imaginary-time-dependent periodic motion of electrons and phonons on the stationary phase of the action derived with the use of Slater determinants. In the strong-coupling limit of both the Holstein and attractive Hubbard models, it reproduces analytically-known effective hopping of a single bipolaron because the tunneling involves only one in this limit. The method gives new results in other general cases and is easily applied to excited or more complex systems.

When dynamics of self-trapped nonlinear excitations is studied, tunneling is often encountered. For example, when a free-exciton state is metastable and separated from a self-trapped-exciton state by a potential barrier, nonradiative processes of trapping excitons occur via tunneling [1]. Another example is low-temperature dynamics of small polarons and bipolarons in the broad sense: they may accompany a lattice distortion, a distortion of spin order [2], or both of them. If they are so small that lattice discreteness is essential, they have to overcome the lattice pinning potential to move around.

Self-trapping is a consequence of many-body effects. It is determined by the balance between the itinerant nature of electrons, the Coulomb interaction, electron-lattice coupling, superexchange coupling between spins, etc. Tunneling rates should be calculated with proper account of spatial and temporal structures of the many-body system during the dynamical process. The length and time scales of charge-density fluctuations are different from those of lattice vibrations and those of spin fluctuations.

In order to treat tunneling in such many-body systems with electrons and phonons, we propose using a time-dependent mean-field theory which is free from constraint on the dynamical paths of self-trapped nonlinear excitations. Specifically, we calculate the effective hopping strength of a self-trapped kink in the one-dimensional extended Peierls-Hubbard model near half filling using the instanton technique [3 ,4]. Imaginary-time transition amplitudes are written in a functional integral form with the use of an overcomplete set of Slater determinants for the electronic part [5] and lattice coordinates and momenta for the phonon part.

Time-dependent mean-field equations are derived by the stationary phase condition with respect to one-body wave functions consisting of Slater determinants and the lattice variables. The electronic part is the imaginary-time-dependent Hartree-Fock (HF) equation. The lattice part corresponds to the Newton equation in the inverted potential. The mean-field solution bouncing between neighboring local minima of the adiabatic HF total energy determines the classical contribution to the action and thus the exponent of the effective hopping. Fluctuations around the mean-field solution determine the prefactor of the effective hopping after Gaussian integration.

It should be noted that tunneling can be treated more generally when constructing classical paths: a theory of spontaneous nuclear fission [6] does not rely on the instanton technique. Here we use Slater determinants instead of Hubbard-Stratonovich auxiliary fields [6] to have the HF equation at the mean-field level [5]. Furthermore, we calculate the prefactor through Gaussian integration over small fluctuations with respect to particle-hole excitations and phonons on an equal footing for the first time. We take proper time-ordering among fluctuation variables: it is important because of the lack of a continuum limit when Slater determinants are used [5]. Fluctuations are treated in the lowest order including the orthonormal condition for the one-body wave functions. This loosens the Fermi statistics and is equivalent to bosonization. Indeed, it can be shown as illustrated in Ref. [7] that, if we treat *real*-time-dependent small fluctuations around the stable *static* mean-field solution, we obtain the linearized excitation modes in the most unrestricted form of the random-phase approximation [8].

Here we take the one-dimensional extended Peierls-Hubbard model:

$$H = \sum_i \left[-t \sum_\sigma (c^\dagger_{i+1\sigma} c_{i\sigma} + c^\dagger_{i\sigma} c_{i+1\sigma}) + U n_{i\uparrow} n_{i\downarrow} + V n_i n_{i+1} - \beta u_i n_i + \frac{K}{2} u_i^2 + \frac{1}{2M} p_i^2 \right] , \qquad (1)$$

where $c^\dagger_{i\sigma}$ ($c_{i\sigma}$) creates (annihilates) an electron with spin σ at site i, $n_{i\sigma} = c^\dagger_{i\sigma} c_{i\sigma}$, $n_i = \sum_\sigma n_{i\sigma}$, u_i and p_i represent the lattice coordinate and its conjugate momentum at site i, respectively. The parameter t denotes the transfer integral, U the on-site repulsion, V the nearest-neighbor repulsion, β the on-site electron-phonon coupling, K the spring constant between ions, and M the ionic mass. The bare phonon frequency is given by $\omega = \sqrt{K/M}$. Dimensionless electron-phonon coupling is defined by $\lambda = \beta^2/(Kt)$.

We take such parameters that the ground state is a charge-density-wave (CDW) state at half filling (i.e., $\beta^2/K - U + 2V \gtrsim 0$). At strong coupling, small bipolarons are formed, each of which consists of a pair of electrons on a site with lattice distortion of about $2\beta/K$. The CDW state at half filling contains a bipolaron on every second site. We remove one electron from a half-filled periodic system with an odd number of sites. There is a place where two consecutive sites are almost empty, which is regarded as a kink or a soliton connecting the two degenerate CDW phases. The kink tunnels into the neighboring equivalent positions at two lattice units' distance so as to form a band of Bloch states with well-defined momenta.

To solve the mean-field equations depending on imaginary time $t = -i\tau$, we first impose a period of motion, $T = -iT_2$ with T_2 being a real number, and then search a self-consistent motion of electrons and phonons during $-T_2/2 \le \tau \le T_2/2$ including initial values at $\tau = -T_2/2$. To obtain the self-consistent motion, we use a method very similar to Ref. [6] for the electronic part. The initial values for the lattice part are determined so that the solution bounces back to the initial state. Because the solution is on a saddle point of the multi-dimensional space-time, we imposed a constraint which vanishes at the saddle point.

At $\tau = -T_2/2$ with T_2 being large enough, the configuration of charge densities and lattice displacements is close to that of a stable static mean-field solution. Around $\tau = -T_2/4$, a bipolaron near the kink is once broken. Then, the charge density and the lattice distortion of the bipolaron flow inside the kink to form another bipolaron. Effectively, the bipolaron is shifted by one lattice unit, and the kink by two lattice units. At $\tau = 0$, the configuration is close to that of another static solution with the different kink location from $\tau = -T_2/2$. The motion after $\tau = 0$ is the reflection of that before $\tau = 0$: the kink bounces back to the original place. The above solution is usually called a bounce, which contains an instanton ($\tau < 0$) and an anti-instanton ($\tau > 0$). The motion occurs locally in space and time.

At the tunneling process around $\tau = \pm T_2/4$, the charge density $\rho_i(\tau)$ varies more rapidly than the lattice displacement scaled by $Ku_i(\tau)/\beta$. As ω increases, their motion becomes faster and the instanton width becomes shorter. The ratio of $K\dot{u}_i(\tau)/\beta$ to $\dot{\rho}_i(\tau)$ (the dot denotes the τ derivative) on the i-th site where the bipolaron tunnels into at $\tau = -T_2/4$ increases with ω and it becomes unity in the $\omega \to \infty$ limit.

By the instanton technique, we get energies of Bloch states which are the same as in the tight-binding model of transfer

$$t_{\rm eff} = \hbar J K e^{-\frac{W_2}{2\hbar}} . \quad (2)$$

The quantity W_2 is the $T_2 \to \infty$ limit of the imaginary part of the reduced action for the bounce solution,

$$W_2[E_{HF}(T_2)] = \int_{-\frac{T_2}{2}}^{\frac{T_2}{2}} d\tau \left(\sum_i p_i(\tau) \frac{\partial}{\partial \tau} u_i(\tau) + \sum_{i,\sigma,\gamma \in {\rm occ}} \phi^*_\gamma(i,\sigma,-\tau) \hbar \frac{\partial}{\partial \tau} \phi_\gamma(i,\sigma,\tau) \right) + \hbar \sum_{\gamma \in {\rm occ}} \lambda_\gamma , \quad (3)$$

where $\phi_\gamma(i,\sigma,\tau)$ is the one-body wave function of orbital γ at site i, spin σ, and time τ, which satisfies periodic boundary condition, $\phi_\gamma(i,\sigma,\frac{T_2}{2}) = e^{-\lambda_\gamma} \phi_\gamma(i,\sigma,-\frac{T_2}{2})$. The last term of (3) cancels this exponent at the boundary, guaranteeing the gauge invariance. The symbol $\gamma \in$ occ means that summation is over occupied orbitals. The factor $W_2/2$ in the exponent of (2) is for the instanton solution ($\tau \le 0$).

The prefactor $\hbar JK$ comes from Gaussian integration over small fluctuations around the instanton solution with the instanton-translating zero-mode excluded in a proper manner [3 ,4]. Note that $W_2[E_{HF}(T_2)]$ has contributions from the lattice motion [the first term in the parenthesis of (3)] and the electronic motion [the rest of (3)]. As ω increases, the absolute value of the exponent $W_2/(2\hbar)$ becomes smaller, the electronic contribution to it becomes more substantial [Fig. 1(a)]. The prefactor $\hbar JK$ is roughly proportional to $\hbar\omega$.

The HF energy $E_{HF}(T_2)$ in (3) is a constant of motion and a decreasing function of the period T_2 [Fig. 1(b)]. In the $T_2 \to \infty$ limit, where the bounce solution starts from the state identical with the static solution, $E_{HF}(T_2)$ is the same as in the static case. As T_2 approaches a critical value T_{2c} from above, $E_{HF}(T_2)$ increases towards that of an *unstable* static mean-field solution on the top of a barrier. Below T_{2c}, there is no time-dependent solution ($W_2[E_{HF}(T_2)] = 0$). Infinitesimally above T_{2c}, the bounce solution corresponds to a small-amplitude harmonic oscillation around the unstable static solution, which has a characteristic period of T_{2c}. Note that T_{2c} decreases with increasing ω because of the shorter instanton width.

The effective hopping $t_{\rm eff}$, calculated through (2), is plotted as a function of λ [Fig. 2(a)] and ω [Fig. 2(b)] for the Holstein model ($U = V = 0$) and as a function of $|U|$ (Fig. 3) for the attractive Hubbard model ($V = \lambda = 0$). It is compared with a strong-coupling analysis below. At strong coupling, bipolarons are tightly bound and the kink is well localized. Only a single bipolaron effectively participates in the tunneling. In this case, the effective hopping can be evaluated by the second-order perturbation theory with respect to t [9 ,10]. Intermediate states have two consecutive singly-occupied sites with phonons excited around the equilibrium position β/K. We define $\tilde{t}$ by the perturbational result obtained by summing over these intermediate states. It can be shown in the Holstein model that $\tilde{t} \simeq \exp[-2\beta^2/(K\omega)]$ at large $\beta^2/(K\omega)$, and $\tilde{t} = 2t^2K/\beta^2$ in the $\omega \to \infty$ limit. Note that this model is reduced, in the $\omega \to \infty$ limit, to the attractive Hubbard model of coupling strength $U_{eff} = -\beta^2/K$ [10], which has $\tilde{t} = 2t^2/|U_{eff}|$. The semiclassical evaluation of $t_{\rm eff}$ shows the correct exponential behavior at large $\beta^2/(K\omega)$ in the Holstein model (Fig. 2). As $|U|$ increases in the attractive Hubbard model, both $W_2/(2\hbar)$ and $\hbar JK$ increase to show the expected inversely proportional behavior at large $|U|$ (Fig. 3).

At weak coupling, bipolarons are loosely bound and the CDW has a smaller amplitude. The kink is delocalized with a coherence length of about v_F/Δ where v_F is the Fermi velocity of the noninteracting system and Δ is a gap in the electronic spectrum at half filling. Due to the weaker binding of bipolarons, the barrier between the stable static mean-field solutions is lowered. The reduced potential energy is converted into the reduced kinetic energy at the top of the barrier (i.e., at the bottom in the inverted potential). It decreases the magnitude of purely imaginary velocities (i.e., electronic current densities and lattice momenta) at the tunneling and thus $W_2/(2\hbar)$ [see (3)]. The kink becomes more mobile.

When the barrier height is more than some fraction of t or ω, motion of the kink is described by the tight-binding model as the dilute-instanton-gas approximation results in. It is valid as far as the instanton density per unit imaginary time, $JKe^{-\frac{W_2}{2\hbar}}$ [4], is so small that multi-instanton configurations, which are summed over in the derivation of (2), nearly satisfy the stationary phase condition. On the other hand, when the barrier is negligible, a continuum approximation becomes valid. Motion of the kink would be described by a free-particle model of mass determined by a collective coordinate method as in field theories (Chap. 8 of Ref. [4]).

The present method is limited to dynamical processes of non-negligible barriers. But, the method is so general that systems can be complex or excited. The above examples of the Holstein and attractive Hubbard models contain only on-site interactions and allow alternative approaches at strong coupling [9 ,11 ,12]. These models are adopted here for the purpose of illustrating how the method works.

Next, the extended Peierls-Hubbard model is studied. At strong coupling ($\lambda \gg 1$), the repulsion U enhances the tunneling of the kink [Fig. 4(a)], meanwhile V suppresses it [Fig. 4(b)]. Here we plot the absolute value of the exponent, $W_2/(2\hbar)$, since the prefactor $\hbar JK$ is affected little. The above behavior is due to the fact that U weakens the binding of bipolarons, but V strengthens it. The U-dependence of the effective hopping is much weaker than a previous analysis of $-\log(\tilde{t}) \simeq 2(\beta^2/K - U)/\omega$ [13]. The effect of U is not described by the replacement $\beta^2/K \rightarrow \beta^2/K - U$ as the half-filled phase diagram indicates. The effective hopping is dominantly determined not by the energies of intermediate states but by the overlaps of displaced phonon wave functions. The latter are much less affected by the repulsion than the former because the lattice distortion is little affected.

In this work, we did not consider multi-kink cases at finite-density doping away from half filling, where we have to consider kink-anti-kink interaction as well as instanton-(anti-)instanton interaction.

Acknowledgments

The author is very grateful to Lu Yu and Zhao-Bin Su for valuable discussions and enlightening comments, A.R. Bishop for his continuous encouragement and C. Castellani for his comment on the lack of a continuum limit. He would also like to thank Professor Abdus Salam, the International Atomic Energy Agency, UNESCO and the International Centre for Theoretical Physics, Trieste, for support.

References

[1] A. S. Ioselevich and E. I. Rashba, in *Quantum Tunneling in Condensed Media*, edited by Yu. Kagan and A. J. Leggett (North-Holland, Amsterdam, 1992).

[2] A. Auerbach and B. E. Larson, Phys. Rev. Lett. **66**, 2262 (1991); A. Auerbach, Phys. Rev. B **48**, 3287 (1993).

[3] S. Coleman, in *The Whys of Subnuclear Physics*, edited by A. Zichichi (Plenum, New York, 1979).

[4] R. Rajaraman, *Solitons and Instantons* (North-Holland, Amsterdam, 1982).

[5] J. W. Negele and H. Orland, *Quantum Many-Particle Systems* (Addison-Wesley, Redwood City, Calif., 1988), Chapter 7.

[6] S. Levit, J. W. Negele, and Z. Paltiel, Phys. Rev. C **22**, 1979 (1980).

[7] S. Levit, J. W. Negele, and Z. Paltiel, Phys. Rev. C **21**, 1603 (1980).

[8] K. Yonemitsu, A. R. Bishop, and J. Lorenzana, Phys. Rev. B **47**, 12059 (1993).

[9] G. Beni, P. Pincus, and J. Kanamori, Phys. Rev. B **10**, 1896 (1974).

[10] J. E. Hirsch and E. Fradkin, Phys. Rev. B **27**, 4302 (1983).

[11] I. G. Lang and Y. A. Firsov, Zh. Eksp. Teor. Fiz. **43** 1843 (1962) [Sov. Phys. JETP **16** 1301 (1963)].

[12] H. Zheng, D. Feinberg, and M. Avignon, Phys. Rev. B **39**, 9405 (1989); **41**, 11557 (1990).

[13] J. E. Hirsch, Phys. Rev. B **31**, 6022 (1985).

Figure Captions

FIG. 1. (a) $W_2[E_{HF}(T_2)]/(2\hbar)$ and (b) $E_{HF}(T_2)$ (relative to that of the static solution), for different ω. Parameters are $t = 1$, $U = V = 0$, and $\lambda = 10$. One electron is removed from the half-filled odd-member ring. The lattice contribution to $W_2[E_{HF}(T_2)]/(2\hbar)$ is also shown in (a).

FIG. 2. $-\log(t_{\rm eff})$, (a) as a function of λ for $\omega = 2$; and (b) as a function of ω for $\lambda = 10$. Parameters are $t = 1$ and $U = V = 0$. One electron is removed from the half-filled odd-member ring. The line shows the strong-coupling result, $-\log(\tilde{t}) \simeq 2\beta^2/(K\omega)$.

FIG. 3. $t_{\rm eff}$ as a function of $-U$. Parameters are $t = 1$ and $V = \lambda = 0$. One electron is removed from the half-filled odd-member ring. The line shows the strong-coupling result, $\tilde{t} = 2t^2/|U|$.

FIG. 4. $W_2/(2\hbar)$ (in the $T_2 \rightarrow \infty$ limit), (a) as a function of U for $V = 0$; and (b) as a function of V for $U = 0$. Parameters are $t = 1$, $\lambda = 10$, and $\omega = 1$. One electron is removed from the half-filled odd-member ring. The line is a guide to the eye.

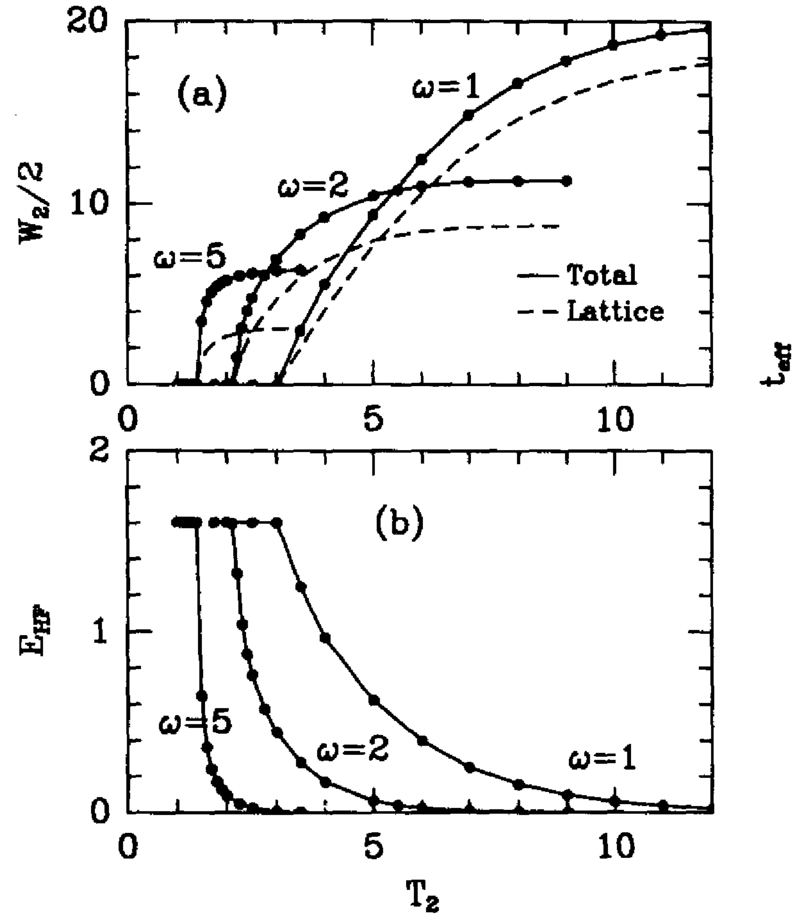
(a)
ω=1
ω=2
ω=5
— Total
-- Lattice
W₂/2
t_eff
(b)
E_HF
ω=5
ω=2
ω=1
T₂

Fig.1

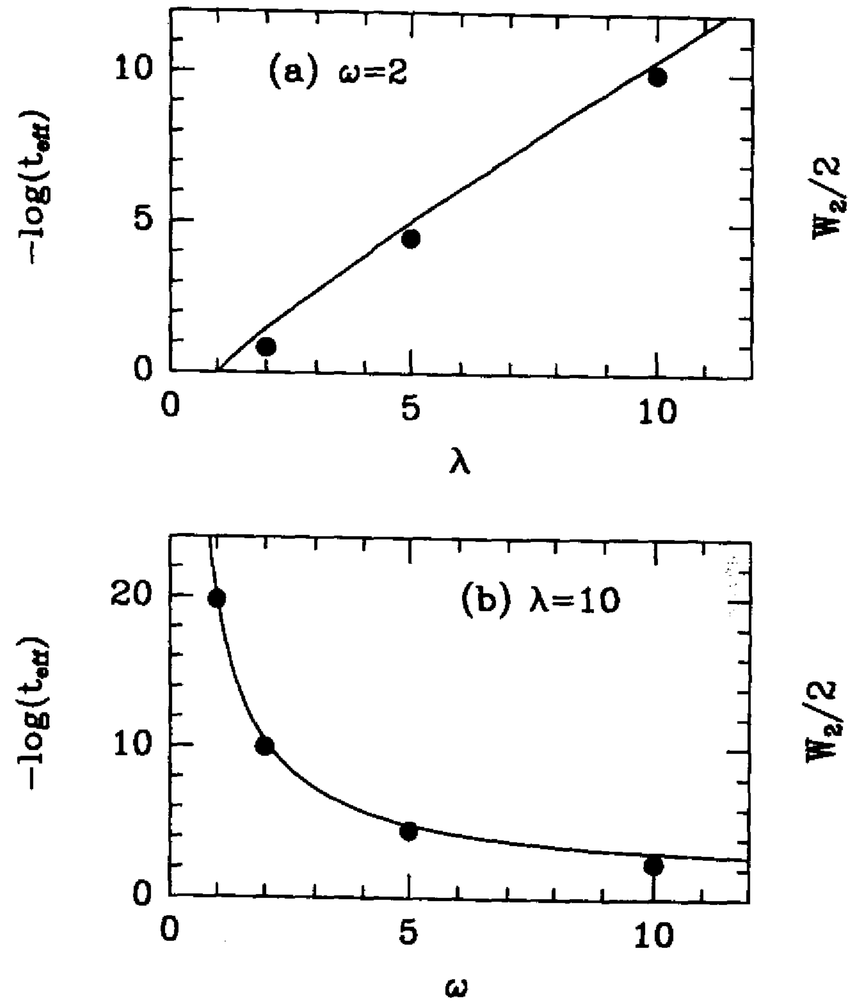
(a) ω=2
−log(t_eff)
W₂/2
λ
(b) λ=10
−log(t_eff)
W₂/2
ω

Fig.2

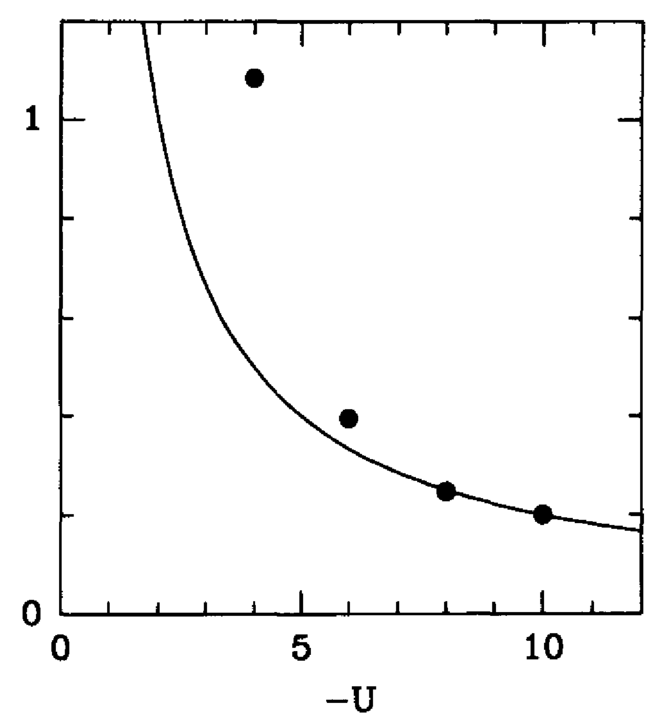

Fig.3

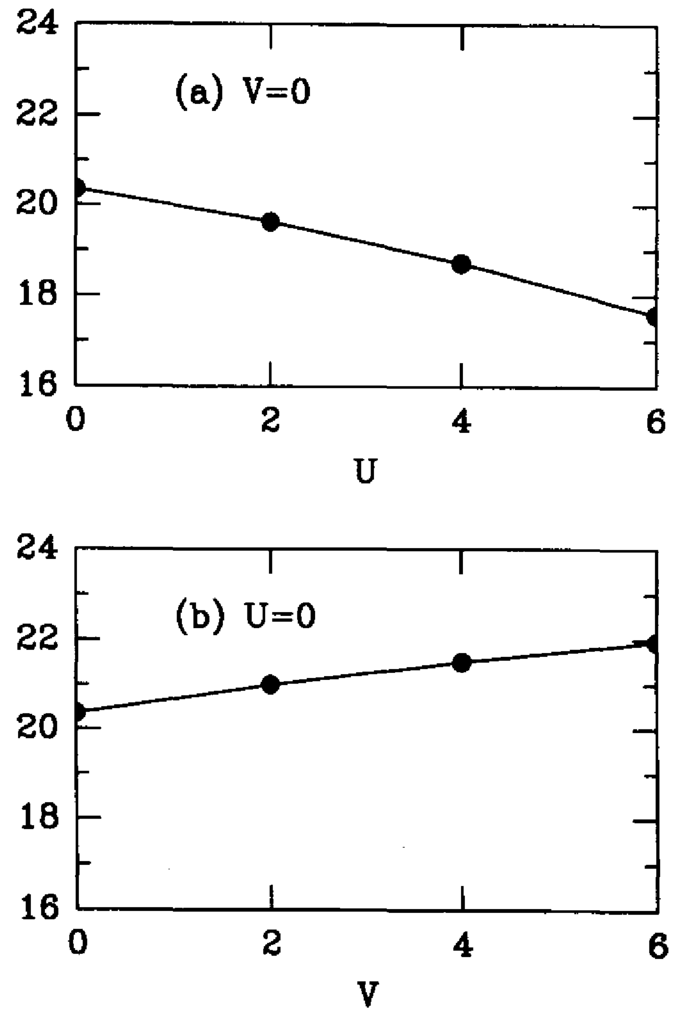

Fig.4